

PERFORMANCE EVALUATION OF FEATURE DETECTION FOR LOCAL OPTICAL FLOW TRACKING

Tobias Senst, Brigitte Unger, Ivo Keller and Thomas Sikora

Communication Systems Group, Technische Universität Berlin, Einsteinufer 17, Berlin, Germany

Keywords: Feature detector, Feature detection Performance evaluation, Tracking, KLT.

Abstract: Due to its high computational efficiency the Kanade Lucas Tomasi feature tracker is still widely accepted and a utilized method to compute sparse motion fields or trajectories in video sequences. This method is made up of a Good Feature To Track feature detection and a pyramidal Lucas Kanade feature tracking algorithm. It is well known that the Good Feature To Track takes into account the Aperture Problem, but it does not consider the Generalized Aperture Problem. In this paper we want to provide an evaluation of a set of alternative feature detection methods. These methods are taken from feature matching techniques like FAST, SIFT and MSER. The evaluation is based on the Middlebury dataset and performed by using an improved pyramidal Lucas Kanade method, called RLOF feature tracker. To compare the results of the feature detector and RLOF pair, we propose a methodology based on accuracy, efficiency and covering measurements.

1 INTRODUCTION

Motion based analysis of a video sequence is an important topic in computer vision and visual surveillance. The KLT feature tracker (Tomasi and Kanade, 1991) still remains as a widely accepted and utilized method to compute sparse motion fields or trajectories in video sequences due to its high computational efficiency (Ali and Shah, 2007; Hu et al., 2008; Fradet et al., 2009). The KLT tracker is based on a GFT (Good Feature To Track) corner detector (Shi and Tomasi., 1994) and the Lucas/Kanade local optical flow method (Lucas and Kanade, 1981).

In the recent past several improvements of the Lucas/Kanade method have been developed: Pyramidal implementation (Bouguet, 2000) was proposed to estimate large motions, parallelizing using the GPU (Sinha et al., 2006) increases the runtime performance drastically, gain adaptive modifications (Zach et al., 2008) extend the robustness against varying illuminations and robust norms in association with a adaptive region size (Senst et al., 2011) improve the robustness against partial occlusion and non Gaussian noise. Whilst the tracking by local optical flow has been improved continually, the feature detecting is still based on the GFT method. This leads to several drawbacks. E.g. the GFT does not consider the multi scale approach of the pyramidal Lucas/Kanade implementation. Even the Lucas/Kanade local con-

stant motion constraint is not taken into account by the GFT algorithm. In the recent decades feature detectors were developed for feature matching methods, e.g. SIFT (Scale Invariant Feature Transform) (Lowe, 1999), SURF (Speeded Up Robust Features) (Bay et al., 2008) and MSER (Maximally Stable Extremal Regions) (Matas et al., 2002). These techniques were applied e.g. in stereo, SLAM (Simultaneous Localization and Mapping) and image stitching applications.

In this paper, we investigate the usability of several feature detectors related to local optical flow tracking. The evaluation is based on the Middlebury dataset (Baker et al., 2009). The dataset provides synthetic and realistic pairs of consecutively captured images and the optical flow as ground truth for each pair. We provide metrics for sparse motion estimation. These metrics take into account the accuracy, efficiency and the covering of the sparse motion field.

2 FEATURE DETECTION

In this section we briefly introduce the set of evaluated feature detectors. Most of the detectors are designed for feature matching, whose requirements differ from the tracking with local optical flow. Feature matching methods associate feature points of different images by extracting descriptors from the detected feature lo-

cation. Thus the features provide a limited set of well localized and individually identifiable anchor points. Important properties are repeatability and invariance against rotation, translation and scaling (Tuytelaars and Mikolajczyk, 2008).

The local optical flow estimates the feature motion by a first order Taylor approximation of the brightness constancy constraint equation of a specified region (Lucas and Kanade, 1981). Thus it depends on the appearance of vertical and horizontal derivatives of the image. This is known as the aperture problem. In addition it constrains that the specified region contains one moving pattern. This extends the aperture problem to the generalized aperture problem (Senst et al., 2011). As a consequence important properties of the patterns close to the feature points detected by a feature detector are cornerness and motion constancy.

Good Features to Track. The GFT method (Shi and Tomasi., 1994) is designed to detect cornerness patterns. The Gradient matrix \mathbf{G} is computed for each pixel as:

$$\mathbf{G} = \sum_{\Omega} \begin{bmatrix} I_x^2 & I_x I_y \\ I_x I_y & I_y^2 \end{bmatrix} \quad (1)$$

with the intensity values $I(x,y)$ of a grayscale image and the spatial derivatives I_x, I_y for a specified region Ω . The gradient matrix is implemented by means of integral images for I_x^2, I_y^2 and $I_x I_y$. Due to the use of integral images the computational complexity of the gradient matrix is constant and independent of the size of Ω . A good feature can be identified by the maxima of $\lambda(x,y)$, the smallest eigenvalue of \mathbf{G} . Thus good features prevent the aperture problem. Certainly strong corners appear at object boundaries, where multiple motions are very likely. This leads to the generalized aperture problem. Post processing is applied by non-maximal suppression and thresholds at $q \cdot \max(\lambda(x,y))$, with q the cornerness quality constant.

Pyramidal Good Features to Track. The PGFT method is the pyramidal extension of the GFT method. The pyramidal implementation is done by up-scaling the region Ω based on integral images. That is more efficient than down-scaling the image. For each scale the smallest eigenvalue $\lambda_s(x,y)$ of the corresponding Gradient matrix is computed. A good feature can be identified by the maxima of $\lambda(x,y)$, whereby:

$$\lambda(x,y) = \max_s (\lambda_s(x,y)) \quad (2)$$

is the maximal eigenvalue of each scale.

Feature from Accelerated Segment Test. The FAST (Rosten and Drummond, 2006) method is de-

signed as runtime efficient corner detector. Corners are assumed at positions with not self-similar patches. This is measured by considering a circle, where I_C is the intensity from the centre of the circle and I_P and $I_{P'}$ are the intensity values on the diameter line through the center and at the circle, hence at opposite positions. Thus a patch is not self-similar if pixels at the circle look different from the centre. The filter response is performed on a Bresenham circle and given by:

$$C = \min_P (I_P - I_C)^2 + (I_{P'} - I_C)^2. \quad (3)$$

Rosten and Drummond proposed a high-speed test to find the minimum in computationally efficient way.

Scale Invariant Feature Transform. The SIFT (Lowe, 1999) method provides features that are translation, rotation and scale invariant. To achieve this, features are selected at maxima and minima of a DoG (Difference of Gaussian) function applied in scale space by building an image pyramid with resampling between each level. Focusing on speed the DoG is used to approximate the LoG (Laplacian of Gaussian). The local maxima or minima are found by comparing the 8 neighbors at the same level. These maxima or minima are compared to the next lowest level of the pyramid.

Speeded Up Robust Features. The SURF (Bay et al., 2008) are designed with a fast scale space method using DoB (Difference of Box) filters as a very basic Hessian matrix approximation. The Hessian matrix \mathbf{H} at each scale is defined as:

$$\mathbf{H} = \begin{bmatrix} I_{xx} & I_{xy} \\ I_{xy} & I_{yy} \end{bmatrix} \quad (4)$$

where I_{xx} is the convolution of the Gaussian second order derivative with the image I . The DoB filters are implemented by integral images, hence the computation time is independent of the filter size. The filter response is defined as the weighted approximated Hessian determinant, where local maxima identify blob like structures. The scale space is analysed by up-scaling the box filter, which is more efficient than down-scaling the image, followed by a scale space non-maximum suppression.

STAR. The STAR detector is derived from the CenSurE (Center Surround Extrema) detector (Agrawal et al., 2008). As well as the SURF the CenSurE is based on box filters. While DoB filters are not invariant to rotation, Agrawal introduced center-surround filters that are bi-level. The STAR feature detector uses a center-surrounded bi-level filter of two rotated

squares. The filter response is computed for seven scales and each pixel of the image. In contrast to SIFT and SURF the sample size is constant on each scale and is leading to a full spatial resolution at every scale. Post processing steps are done by non-maximal and line suppression. Features that lie along an edge or line are detected due to the Gradient matrix, see Eq. 1.

Maximal Stable Extremal Regions. The MSER detector (Matas et al., 2002) is designed to detect affine invariant subsets of maximal stable extremal regions. MSER are detected by consecutively binarizing an image by a threshold. The threshold is applied from the maximal image intensity value to its minimal. At each step a set of regions Φ is computed by connected components analysis. The filter response for each region i is defined as:

$$q_i = |\Phi_{i+\Delta} \setminus \Phi_{i-\Delta}| / |\Phi_i| \quad (5)$$

where $|\dots|$ denotes the cardinality and $i \pm \Delta$ the region at Δ th lower or higher threshold level. The MSER are identified by the local minimum of q .

3 FEATURE TRACKING

The motion estimation of the detected features is performed using RLOF (Robust Local Optical Flow) method (Senst et al., 2011) which is derived from the pyramidal Lucas/Kanade method (Bouguet, 2000). Based on the spatial and temporal derivatives of a specified region Ω the RLOF computes the feature motion using a robust regression framework. A robust redescending composed quadratic norm was introduced to increase the robustness of motion estimation compared to pyramidal Lucas/Kanade method. To improve the behaviour at motion boundaries an adaptive region size strategy is applied to decrease Ω . The region Ω of a feature is decreased until the feature is trackable or a minimal region size is reached. The decision of being trackable is done by analysing the smallest eigenvalue λ , see Section 2, and the residual error of the motion estimates.

For the experiment the following parameters are used: a minimal region size of 7×7 , a maximal region size of 15×15 , the robust norm parameters $\sigma_{1/2} = (8, 50)$, 3 levels and maximal 20 iterations. The RLOF is performed bidirectional, thus incorrect tracked features could be detect. We identify these by checking the consistency of forward and backward flow using a threshold $\varepsilon_d = 1$:

$$\|\mathbf{d}_{I(t) \rightarrow I(t+1)} + \mathbf{d}_{I(t+1) \rightarrow I(t)}\| < \varepsilon_d \quad (6)$$

where $I(t) \rightarrow I(t+1)$ denote the forward motion and $I(t+1) \rightarrow I(t)$ the reverse.

4 EVALUATION METHODOLOGY

The Middlebury dataset (Baker et al., 2009) has become an important benchmark regarding dense optical flow evaluation. It provides synthetic and realistic pairs of consecutively captured images. The ground truth is given by optical flow for each pair. We use the database to evaluate the sparse optical flow results of the features found by the respective detector and tracked with the RLOF. We refine the evaluation methodology of Baker *et al.* (Baker et al., 2009) in terms of accuracy, efficiency and covering measures. For each algorithm and each sequence we record the T_D the set of detected features, $T_T \subset T_D$ the set of tracked trajectories with \dot{x}_T the endpoint of each trajectory as well as the runtime. The respective ground truth motion is given by $\dot{x}_{T_{GT}}$ the ground truth endpoint of each trajectory.

Accuracy Measures. A basic property is the accuracy of the estimated tracks. The most commonly used measure is the endpoint error (Otte and Nagel, 1994) defined by:

$$EE(\dot{x}_T) = \|\dot{x}_T - \dot{x}_{T_{GT}}\|^2. \quad (7)$$

The compact statistic of the EE is often only given by the averages. Thus the measurement is affected by the outliers. Baker *et al.* proposed robust statistics by applying a set of thresholds to the error measurements. This report is limited so we decide to use the Median of endpoint errors (MEE).

Efficiency Measures. We measure the feature detection runtime t_D , which describes the computational complexity of the detection method and the tracking efficiency is defined as:

$$\eta = \frac{|T_T|}{|T_{GT}|}. \quad (8)$$

In most cases the computational complexity of feature tracking is dominant. Therefore the tracking efficiency is an important measurement to trace methods detecting features which produce small MEE but a large number of rejected trajectories. Finally the t denotes the overall detection and tracking runtime.

Covering Measures. Compared with the evaluation of a dense optical flow method the challenge of comparing methods producing sparse motion fields is not

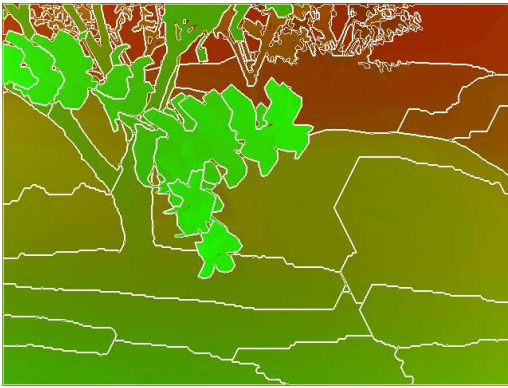


Figure 1: Ground truth optical flow and motion segments of the Grove2 sequence (The optical flow is shown as color-code).

only to compare the outliers and the accuracy of the resulting track, but also to compare whether all the moving objects are assigned to tracks. In particular it depends on the application. For example methods as SLAM (Jonathan and Zhang, 2007) or GME (Tok et al., 2011) use trajectories of the background. In these examples it is not critical if the set of trajectories does not include all foreground objects. But for applications of motion based image retrieval e.g. object segmentation or extraction (Brostow and Cipolla, 2006) all objects have to be covered by trajectories. The covering measurement ρ is motivated by measuring the ability of the sparse motion field to represent all different moving objects in a scene. At first the ground truth is divided into a set of similar moving regions C by the color structure code segmentation method. This algorithm (Rehrmann and Priebe, 1997) is modified to deal with a 2D motion field, see Figure 1. For each region C the density is computed as the quotient of the number of tracks $|T_T \subset C|$ located at C and the area A_C of the region. The covering measurement ρ is defined as the mean density.

$$\rho = \frac{1}{|C|} \sum_{|C|} \frac{|T_T \subset C|}{A_C} \quad (9)$$

5 EVALUATION RESULTS

In this paper our goal is to provide a set of baseline results to allow researchers to get a feel for a feature detector that has a good performance on their specific problem. For this purpose we evaluate the proposed detection methods at the operating point of around 200 and 2500 feature points. We choose the operating point of around 200 points to analyze the performance of the feature detector with few feature points. Particularly in that case an ideal detector should provide a

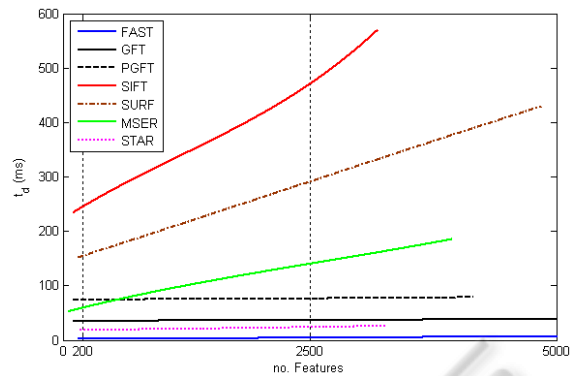


Figure 2: Feature detection runtime t_d related to the number of detected features for the *Grove3* sequence with VGA resolution.

high tracking performance, which indicates that the features are not set to motion boundaries where they are rejected more likely by the tracker. In contrast we want to analyze the performance regarding to the coverage with a denser motion field of around 2500 feature points.

The results for all algorithms are shown in Table 1. The experiments are performed on an AMD Phenom II X4 960 running at 2.99 GHz. All feature detections are computed on the CPU. The feature tracking is implemented by the RLOF method running on a Nvidia GTX 480 graphic device. The results suggest the following conclusions:

FAST. The FAST detector is designed as a high speed runtime efficient corner detector, which our experiments confirm. For the 640×480 *Grove3* sequence the features detection runtime takes only 2 ms. Figure 2 shows that t_d is nearly constant regarding to the number of detected features. The plain parameterization is an additional advantage of this detector. Summarizing the FAST detector is a very fast detector for a huge set of features with a uniform distribution regarding to the moving object.

GFT. The GFT is the third fastest detector in our benchmark. The runtime t_d is constant regarding to the number of detected features except for a small growing effort of sorting the features. For a small set of features the GFT has the best coverage rate at the *Grove2* and *Grove3*, where the texture is distributed uniformly. At the *Urban2* and *Urban3* the detector achieve the best MEE. However it becomes very inefficient when sequences include a large set of strong edges lying at motion boundaries. These features cannot be tracked. The GFT is a fast and reliable feature detector at standard scenarios. But it should be used with caution at sequences with occlusion and homogeneous objects.

Table 1: Evaluation results for the Middlebury dataset for approximate 200 feature points (left), 2500 feature points (right). Measurements are t_D detection time, t detection and tracking time, η tracking performance, MEE median of endpoint error and ρ mean feature density per motion segment.

	Method	t_D (ms)	t (ms)	η (%)	MEE	ρ (%)		Method	t_D (ms)	t (ms)	η (%)	MEE	ρ (%)
Grove2	GFT	35	98	2.3	0.113	0.42		GFT	37	112	2.0	0.069	1.03
	PGFT	75	138	1.9	0.114	0.42		PGFT	77	156	1.5	0.073	0.90
	FAST	2	63	1.5	0.108	0.30		FAST	4	73	2.1	0.077	2.10
	SIFT	240	304	3.9	0.082	0.26		SIFT	508	588	3.1	0.090	1.04
	SURF	156	215	5.1	0.116	0.12		SURF	280	355	2.3	0.079	0.72
	STAR	18	76	8.7	0.152	0.22		STAR	24	98	2.6	0.082	0.84
	MSER	63	124	4.8	0.094	0.18		MSER	142	215	2.2	0.071	1.62
	Method	t_D (ms)	t (ms)	η (%)	MEE	ρ (%)		Method	t_D (ms)	t (ms)	η (%)	MEE	ρ (%)
Grove3	GFT	35	100	6.7	0.168	0.07		GFT	37	113	7.7	0.099	0.35
	PGFT	74	135	8.0	0.165	0.07		PGFT	77	158	7.3	0.097	0.34
	FAST	2	64	6.2	0.147	0.03		FAST	4	77	9.6	0.138	0.59
	SIFT	251	318	5.2	0.099	0.06		SIFT	522	605	9.0	0.129	0.36
	SURF	151	212	5.4	0.150	0.01		SURF	282	358	8.4	0.129	0.40
	STAR	19	80	9.7	0.134	0.05		STAR	24	99	8.4	0.151	0.31
	MSER	60	123	14.2	0.210	0.02		MSER	148	228	9.5	0.110	0.35
	Method	t_D (ms)	t (ms)	η (%)	MEE	ρ (%)		Method	t_D (ms)	t (ms)	η (%)	MEE	ρ (%)
Urban2	GFT	35	98	11.8	0.084	0.12		GFT	36	117	12.2	0.103	0.64
	PGFT	75	135	11.8	0.085	0.12		PGFT	76	159	12.6	0.101	0.59
	FAST	2	59	14.6	0.104	0.13		FAST	5	78	8.6	0.103	1.18
	SIFT	257	320	4.4	0.103	0.04		SIFT	506	584	11.8	0.104	0.62
	SURF	158	219	8.1	0.177	0.19		SURF	286	364	10.3	0.126	0.83
	STAR	19	78	18.6	0.207	0.05		STAR	24	99	10.7	0.105	0.63
	MSER	54	115	16.2	0.154	0.07		MSER	104	173	9.8	0.107	0.62
	Method	t_D (ms)	t (ms)	η (%)	MEE	ρ (%)		Method	t_D (ms)	t (ms)	η (%)	MEE	ρ (%)
Urban3	GFT	35	101	11.6	0.057	0.12		GFT	36	114	13.9	0.089	0.45
	PGFT	74	134	9.5	0.062	0.19		PGFT	77	161	12.2	0.085	0.48
	FAST	2	59	11.3	0.063	0.21		FAST	5	76	9.1	0.071	0.82
	SIFT	272	336	6.6	0.066	0.07		SIFT	534	616	12.5	0.110	0.54
	SURF	158	216	10.4	0.107	0.13		SURF	300	382	11.5	0.100	0.56
	STAR	18	78	9.1	0.089	0.22		STAR	25	102	10.7	0.081	0.59
	MSER	51	112	19.7	0.127	0.06		MSER	94	158	18.0	0.100	0.34
	Method	t_D (ms)	t (ms)	η (%)	MEE	ρ (%)		Method	t_D (ms)	t (ms)	η (%)	MEE	ρ (%)
RubberWhale	GFT	26	77	2.2	0.055	0.06		GFT	27	89	3.2	0.057	0.99
	PGFT	55	106	1.8	0.059	0.07		PGFT	56	119	3.2	0.057	1.12
	FAST	1	50	0.5	0.051	0.08		FAST	4	63	2.2	0.050	1.25
	SIFT	183	233	1.1	0.129	0.08		SIFT	414	476	1.9	0.057	0.78
	SURF	113	162	4.3	0.180	0.11		SURF	237	299	3.3	0.066	1.06
	STAR	13	62	3.3	0.127	0.10		STAR	18	74	2.0	0.057	0.94
	MSER	51	101	3.0	0.075	0.24		MSER	93	148	2.3	0.051	0.54
	Method	t_D (ms)	t (ms)	η (%)	MEE	ρ (%)		Method	t_D (ms)	t (ms)	η (%)	MEE	ρ (%)
Venus	GFT	18	65	0.6	0.205	0.16		GFT	20	76	6.6	0.225	1.40
	PGFT	38	82	1.7	0.208	0.17		PGFT	40	97	7.1	0.235	1.14
	FAST	1	43	4.5	0.202	0.20		FAST	4	57	4.1	0.204	2.28
	SIFT	128	171	1.5	0.188	0.17		SIFT	267	319	5.3	0.202	0.83
	SURF	80	122	2.5	0.185	0.13		SURF	218	276	4.9	0.202	1.67
	STAR	9	52	3.3	0.210	0.21		STAR	12	60	4.2	0.227	0.75
	MSER	33	76	4.8	0.183	0.16		MSER	62	108	5.6	0.189	0.67
	Method	t_D (ms)	t (ms)	η (%)	MEE	ρ (%)		Method	t_D (ms)	t (ms)	η (%)	MEE	ρ (%)
Hydrangea	GFT	26	80	0.4	0.283	0.42		GFT	27	93	4.7	0.091	1.24
	PGFT	54	106	0.0	0.306	0.42		PGFT	57	124	3.6	0.090	1.27
	FAST	1	50	0.5	0.252	0.25		FAST	5	68	2.6	0.271	3.30
	SIFT	177	228	1.7	0.260	0.24		SIFT	411	484	5.7	0.117	1.51
	SURF	115	165	3.9	0.261	0.47		SURF	257	324	4.6	0.102	1.20
	STAR	13	62	3.1	0.279	0.33		STAR	18	80	3.1	0.105	1.34
	MSER	40	90	1.5	0.303	0.54		MSER	89	151	3.0	0.260	2.70
	Method	t_D (ms)	t (ms)	η (%)	MEE	ρ (%)		Method	t_D (ms)	t (ms)	η (%)	MEE	ρ (%)
Dimetrodon	GFT	25	77	0.00	0.049	0.018		GFT	27	92	0.5	0.138	0.23
	PGFT	54	104	0.00	0.057	0.017		PGFT	56	122	0.6	0.138	0.21
	FAST	1	49	0.00	0.046	0.017		FAST	4	62	0.1	0.058	0.19
	SIFT	178	230	0.00	0.052	0.019		SIFT	375	438	1.0	0.085	0.16
	SURF	113	161	0.00	0.078	0.015		SURF	247	310	0.4	0.102	0.21
	STAR	13	62	0.00	0.051	0.020		STAR	18	75	0.6	0.119	0.17
	MSER	45	96	0.50	0.056	0.017		MSER	59	109	0.2	0.059	0.05

PGFT. The PGFT improves the GFT in some sequence. E.g. *Urban3*, *RubberWhale* and *Hydrangea*, there the tracking efficiency is decreased and the cov-

erage is increased. However, the benefit results in an increased detection runtime.

STAR. Due to the efficient implementation the STAR method reaches the runtime ranking two. In some special sequences as *Venus* or *Urban3* it gets good covering performance with a low feature set. But generally the performance of the STAR is below average.

SIFT. As shown in Figure 2 the SIFT detector runtime depends on the number of features. It is the slowest of the evaluation. But it shows good performance within a low feature set. This method reaches the best MEE results at *Grove2* and *Grove3* and the best tracking performance at the difficult *Urban2* and *Urban3*. In our experiments the scale space analysis of the DoG of the SIFT tends to detect less features at object boundaries. Almost homogeneous regions are also selected, e.g. the sky of the *Grove3* sequence where tracking is still applicable. Though the set of objects are not covered uniformly, this results into low coverage. Summarizing the SIFT detector is a slow feature detector with a high tracking performance at sequences with few objects.

SURF. In our experiments the improved runtime performance regarding the SIFT could be confirmed, but t_d is still high compared to the other detectors. Related to SIFT the SURF shows some improvements at large sets of features in terms of tracking performance and accuracy. But FAST and GFT are still superior at large feature sets.

MSER. The MSER is the only method based on segmentation instead of finding features using first or second order derivatives. In our experiments we could observe that features are less likely detected at object boundaries e.g. in the *RubberWhale* sequence features are detected in the center of the fence holes instead of their corners. Considering the generalized aperture problem this is an important benefit. But it is not reflected in the results of the whole dataset, where the MSER detector achieve average results. Even at the *Venus* sequence it performs the best MEE results.

This sequence is also a challenging sequence for the GFT because it mainly consists of homogeneous objects. Most of the cornerness regions are distributed at the object boundaries. Thus MSER and also the scale space detector SIFT and SURF achieve good results. That leads to the conclusion that a region based or a scale space based approach would be attractive to improve the GFT method.

6 CONCLUSIONS

In this paper we evaluate different feature detectors in conjunction with the RLOF local optical flow method. While the state-of-the-art KLT-Tracker operates with

the GFT detector, our goal is to provide a set of baseline results for alternative feature detectors to allow researchers to get a sense of which detector to use for a good performance on their specific problem. To compare the resulting sparse motion fields we propose a methodology based on accuracy, efficiency and covering measurements. The benchmark is performed on the Middlebury dataset, which provides a set of consecutively captured images and the corresponding dense motion ground truth.

We observe that the efficient performing algorithm is the FAST approach. With a runtime of about 3 ms for a VGA sequence and an overall good performance for the tracking efficiency, median endpoint error and coverage it outperforms the standard GFT detector. For standard scenarios i.e. uniform texture distribution the GFT is a fast and reliable feature detector. From the results given by the evaluations we conclude that for specific sequences, e.g. sequences including homogeneous objects, where the texture distribution concentrates on object boundaries, there is still room for improvements. Limited advantages shows the PGFT but also SIFT and MSER shows enhanced performance under these conditions. Furthermore an improved GFT method could benefit from the scale space analysis of the SIFT or the region based approach of the MSER.

ACKNOWLEDGEMENTS

The research leading to these results has received funding from the European Community's FP7 under grant agreement number 261743 (NoE VideoSense).

REFERENCES

- Agrawal, M., Konolige, K., and Blas, M. (2008). Censure: Center surround extremas for realtime feature detection and matching. In *European Conference on Computer Vision (ECCV 2008)*, pages 102–115.
- Ali, S. and Shah, M. (2007). A lagrangian particle dynamics approach for crowd flow segmentation and stability analysis. In *Computer Vision and Pattern Recognition (CVPR 2007)*, pages 1–6.
- Baker, S., Scharstein, D., Lewis, J., Roth, S., Black, M. J., and Szeliski, R. (2009). A database and evaluation methodology for optical flow. Technical report MSR-TR-2009-179, Microsoft Research.
- Bay, H., Ess, A., Tuytelaars, T., and Gool, L. V. (2008). Surf: Speeded up robust features. *Computer Vision and Image Understanding*, 110(3):346–359.
- Bouguet, J.-Y. (2000). Pyramidal implementation of the lucas kanade feature tracker. Technical report, Intel Corporation Microprocessor Research Lab.

- Brostow, G. and Cipolla, R. (2006). Unsupervised bayesian detection of independent motion in crowds. In *Computer Vision and Pattern Recognition (CVPR 2006)*, pages 594–601.
- Fradet, M., Robert, P., and Pérez, P. (2009). Clustering point trajectories with various life-spans. In *Conference for Visual Media Production (CVMP 2009)*, pages 7–14.
- Hu, M., Ali, S., and Shah, M. (2008). Detecting global motion patterns in complex videos. In *International Conference on Pattern Recognition (2008)*, pages 1 – 5.
- Jonathan and Zhang, H. (2007). Quantitative evaluation of feature extractors for visual slam. In *Canadian Conference on Computer and Robot Vision (CRV 2007)*, pages 157–164.
- Lowe, D. (1999). Object recognition from local scale-invariant features. In *International Conference on Computer Vision (ICCV 1999)*, pages 1150–1157.
- Lucas, B. D. and Kanade, T. (1981). An iterative image registration technique with an application to stereo vision. In *International Joint Conference on Artificial Intelligence (IJCAI 1981)*, pages 674–679.
- Matas, J., Chum, O., Urban, M., and Pajdla, T. (2002). Robust wide baseline stereo from maximally stable extremal regions. In *British Machine Vision Conference (BMVC 2002)*, pages 384–393.
- Otte, M. and Nagel, H.-H. (1994). Optical flow estimation: Advances and comparisons. In *European Conference on Computer Vision (ECCV 1994)*, pages 49–60.
- Rehrmann, V. and Prieese, L. (1997). Fast and robust segmentation of natural color scenes. In *Asian Conference on Computer Vision (ACCV 1997)*, pages 598–606.
- Rosten, E. and Drummond, T. (2006). Machine learning for high-speed corner detection. In *European Conference on Computer Vision (ECCV 2006)*, pages 430–443.
- Senst, T., Eiselein, V., Heras Evangelio, R., and Sikora, T. (2011). Robust modified L2 local optical flow estimation and feature tracking. In *IEEE Workshop on Motion and Video Computing (WMVC 2011)*, pages 685–690.
- Shi, J. and Tomasi, C. (1994). Good features to track. In *Computer Vision and Pattern Recognition (CVPR 1994)*, pages 593 –600.
- Sinha, S. N., Frahm, J.-M., Pollefeys, M., and Genc, Y. (2006). Gpu-based video feature tracking and matching. Technical report 06-012, UNC Chapel Hill.
- Tok, M., Glantz, A., Krutz, A., and Sikora, T. (2011). Feature-based global motion estimation using the helmholtz principle. In *International Conference on Acoustics Speech and Signal Processing (ICASSP 2011)*, pages 1561–1564.
- Tomasi, C. and Kanade, T. (1991). Detection and tracking of point features. Technical report CMU-CS-91-132, CMU.
- Tuytelaars, T. and Mikolajczyk, K. (2008). Local invariant feature detectors: a survey. *Foundations and Trends in Computer Vision Graphics Vision.*, 3:177–280.
- Zach, C., Gallup, D., and Frahm, J. (2008). Fast gain-adaptive klt tracking on the gpu. In *Visual Computer Vision on GPUs workshop (CVGPU 08)*, pages 1–7.